

Effect of substitution on molecular conformation and packing features in a series of aryl substituted ethyl-6-methyl-4-phenyl-2-thioxo-1,2,3,4-tetrahydropyrimidine-5-carboxylates†

Susanta K. Nayak,^a K. N. Venugopala,^a Deepak Chopra,^{*b} Vasu^c and T. N. Guru Row^a

Received 21st September 2009, Accepted 6th November 2009

First published as an Advance Article on the web 9th December 2009

DOI: 10.1039/b919648j

The supramolecular structures of eight aryl protected ethyl-6-methyl-4-phenyl-2-thioxo-1,2,3,4-tetrahydropyrimidine-5-carboxylates were analyzed in order to understand the effect of variations in functional groups on molecular geometry, conformation and packing of molecules in the crystalline lattice. It is observed that the existence of a short intra-molecular C–H... π interaction between the aromatic hydrogen of the aryl ring with the isolated double bond of the six-membered tetrahydropyrimidine ring is a key feature which imparts additional stability to the molecular conformation in the solid state. The compounds pack *via* the cooperative involvement of both N–H...S=C and N–H...O=C intermolecular dimers forming a sheet like structure. In addition, weak C–H...O and C–H... π intermolecular interactions provide additional stability to the crystal packing.

Introduction

The logic of chemical reactivity¹ and selectivity has found application in the rational design of a variety of drug and drug intermediates of immense benefit to mankind. The discovery of a “lead” compound is a laborious process but finds potential applications in the field of medicinal chemistry and is an active area of interest.^{2,3} Molecules containing diverse functional groups and skeletal frameworks have been synthesized and screened for potential biological activity. One such class of compounds is the “Bignelli compounds”. These are poly-functionalized dihydropyrimidine (DHPM’s) exhibiting a broad range of therapeutic and pharmacological properties,⁴ namely, antiviral,⁵ antimimetic,⁶ anticarcinogenic,⁷ antihypertensive⁸ and calcium channel modulators.⁹ Bignelli products containing boronic acid moieties find potential application in the early inhibition of breast cancer cells.¹⁰

Bignelli chemistry has also been utilized for the synthesis of a diverse library of molecules containing the DHPM molecular scaffold, utilizing the 1,2,3-triazole pharmacophore.¹¹ A series of DHP’s (dihydropyrimidines) have been synthesized to understand the role of structure and molecular conformation for modulation of calcium channel function.^{9,12}

Because of similarity in the chemical structure of DHP’s with DHPM’s, intense research has been carried out to understand structure–activity relationships wherein the flexibility associated

with the dihydropyrimidine or dihydropyridine ring plays an important role for the observed biological activity.^{13–15} This subject has been extensively reviewed by Kappe.¹⁶ The crystal and molecular structures of aryl substituted analogs (functionalization of the phenyl ring) have been synthesized and their supramolecular features analyzed in the literature.¹⁷ DHPM’s of this type exhibit conformational flexibility whereby the aryl ring and the ester group can rotate independent of each other and the conformation of the tetrahydropyrimidine ring can change.^{18,19} In view of the tremendous application of this class of compounds, we have synthesized a small library of compounds wherein the ethyl-6-methyl-4-phenyl-2-thioxo-1,2,3,4-tetrahydropyrimidine-5-carboxylate core is constant, and have undertaken to investigate the role of functional groups on molecular geometry, conformation and generation of supramolecular assemblies in the solid state. In this regard, the understanding of molecular recognition processes enables a better understanding of the physical and chemical properties of the solid. It is a cooperative interplay amongst both strong hydrogen bonds and weak intermolecular interactions which dictate overall packing in the crystal lattice. Furthermore, the synthesized compounds have also been evaluated for their antibacterial, *in vitro* antioxidant, and *in vitro* anti-inflammatory pharmacological activity by agar diffusion, and the Bovine Serum Albumin method respectively.²⁰

Experimental

Synthesis

A mixture of ethylacetoacetate (0.1 mol), *monodiltri* substituted benzaldehyde (0.1 mol) and thiourea were refluxed in 50.0 mL of ethanol for 2.0 h in presence of concentrated hydrochloric acid as catalyst (Fig. 1). The reaction completion was monitored through thin layer chromatography and the contents of the reaction mixture was poured into ice-cold water. The precipitate

^aSolid State and Structural Chemistry Unit, Indian Institute of Science, Bangalore, 560012, India

^bIndian Institute of Science Education and Research, ITI (Gas Rahat Building), Govindpura, Bhopal, 462023, India. E-mail: dchopra@iiserbhopal.ac.in; Fax: +0755-4092392; Tel: +0755-4092321

^cVivekananda Degree College, Bangalore, 560 055, India

† Electronic supplementary information (ESI) available: Melting points, yields, relevant geometrical data, IR and NMR data, PXRD and simulated Powder X-ray data. CCDC reference numbers 732834–732838, 734014, 734015, 738484. For ESI and crystallographic data in CIF or other electronic format see DOI: 10.1039/b919648j

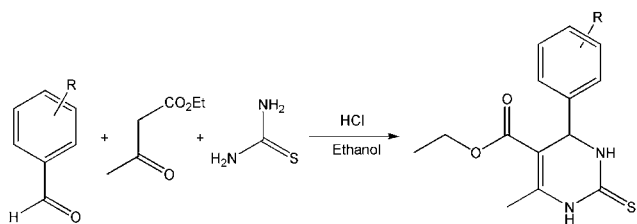


Fig. 1 Chemical scheme of the studied compounds: [PYR1] R = *p*-F; 4-(4-Fluoro-phenyl)-6-methyl-2-thioxo-1,2,3,4-tetrahydro-pyrimidine-5-carboxylic acid ethyl ester. [PYR2] R = *o*-Cl; 4-(2-Chloro-phenyl)-6-methyl-2-thioxo-1,2,3,4-tetrahydro-pyrimidine-5-carboxylic acid ethyl ester. [PYR3] R = *m*-Cl; 4-(3-Chloro-phenyl)-6-methyl-2-thioxo-1,2,3,4-tetrahydro-pyrimidine-5-carboxylic acid ethyl ester. [PYR4] R = *p*-CH₃; 6-methyl-4-(4-methyl-phenyl)-2-thioxo-1,2,3,4-tetrahydro-pyrimidine-5-carboxylic acid ethyl ester. [PYR5] R = *p*-NMe₂; 4-[4-(dimethylamino)phenyl]-6-methyl-2-thioxo-1,2,3,4-tetrahydro-pyrimidine-5-carboxylic acid ethyl ester. [PYR6] R = *p*-OMe; 4-[4-methoxyphenyl]-6-methyl-2-thioxo-1,2,3,4-tetrahydro-pyrimidine-5-carboxylic acid ethyl ester. [PYR7] R = *m*-OMe; 4-[3-methoxyphenyl]-6-methyl-2-thioxo-1,2,3,4-tetrahydro-pyrimidine-5-carboxylic acid ethyl ester. [PYR8] R = *tris*-(OMe)₃; 6-methyl-2-thioxo-4-(3,4,5-trimethoxyphenyl)-1,2,3,4-tetrahydro-pyrimidine-5-carboxylate ethyl ester.

obtained was filtered, dried and crystallized from methanol to obtain the pure compounds. The purity of some of these samples were analyzed through melting point measurements (Table S1[†]), infrared spectroscopic data,²⁰ ¹H-NMR,²⁰ LC-MS.²⁰ Furthermore, powder X-ray (PXRD) data were collected and compared with the simulated powder data obtained from single crystal data (See ESI[†]) thereby proving that the single crystal is representative of the bulk compound.

Data collection, reduction and refinement

A single crystal of [PYR 1, 3, 4, 5, 6, 8] that is of suitable size for single-crystal X-ray diffraction was selected and data were collected on a Bruker AXS SMART APEX CCD diffractometer.²¹ The X-ray generator was operated at 50 kV and 35 mA using Mo-K α radiation ($\lambda = 0.71073 \text{ \AA}$). Data were collected with ω scan width of 0.3°. A total of 606 frames were collected in four different settings of ϕ (0°, 90°, 180°, 270°) keeping the sample to detector distance fixed at 6.03 cm and the 2θ value fixed at -25°. The data were reduced using SAINTPLUS and an empirical absorption correction was applied using the package SADABS.²⁰ The remaining crystals [PYR 2, 7] were recollected in CrysAlis CCD, Oxford Diffraction with an X-ray generator at 49.30 kV and 0.980 mA, using Mo-K α radiation ($\lambda = 0.7107 \text{ \AA}$).²¹ The cell refinement, the data reduction was done in CrysAlis RED.²² The structures were solved by direct methods using SHELXL97²³ present in the program suite WinGX (version 1.70.01).²⁴ The molecular diagrams were generated from ORTEP-32²⁵ and the packing diagrams were generated using Mercury.²⁶ Geometrical calculations were done using PARST95²⁷ and PLATON.²⁸ The non-hydrogen atoms are refined anisotropically and hydrogen atoms bonded to C and N atoms were positioned geometrically and refined using a riding model with distance restraints of N-H = 0.86 Å, aromatic C-H = 0.93 Å, methyl C-H = 0.96 Å and with $U_{\text{iso}}(\text{H}) = 1.2U_{\text{eq}}(\text{N,C})$ and $1.5U_{\text{eq}}(\text{N,C})$.

Results

The molecular and crystal structures of all the eight compounds (PYR1–8) have been determined at room temperature. The solid state molecular geometry were optimized for all the compounds using the Gaussian03 program package,²⁹ using B3LYP conjunction with the 6-31G** basis sets. Structures were visualized in the software MERCURY.²⁶ It is noteworthy that all the relevant torsion angles obtained from experiment and theory are comparable with each other, except for C14–C9–C4–C3, its magnitude depicting the rotational twist of the phenyl ring with respect to the six-membered tetrahydropyrimidine ring.

Fig. 1 depicts the chemical scheme of all the compounds under investigation. Table 1 lists the relevant crystallographic data and the relevant torsion angles affected by functional group substitution, obtained from experiment are listed in Table 2. Table 3 lists all the intra- and intermolecular interactions observed in all the crystal structures.

The relevant bond lengths and bond angles are given in Table S2.† Table S3† lists the Cremer and Pople parameters³⁰ for the 6-membered rings, Table S4† lists the dihedral angles between the aryl ring with the tetrahydropyrimidine and carboxylic acid moiety. Table S5† lists the deviation of the flagpole atoms C4 and N1 from the least squares plane passing through N2, C1, C2, and C3. The list of torsion angles obtained from theory at the B3LYP/6-31G** are listed in Table S6.†

Structure of PYR1

The compound crystallizes in the triclinic space group $P\bar{1}$ with $Z = 2$ molecules in the unit cell [Fig. 2]. It exists in the twist-boat conformation with C4 and N1 forming the flagpole atoms. The carbonyl group C5=O1 exists in an *s-trans* conformation with respect to the C2–C3 double bond and is non planar with the six membered dihydropyrimidine ring, the dihedral twist being 26.10(2)°. It is noteworthy that an intramolecular C–H \cdots π interaction is present in the existing molecular conformation, between H14 and the C2=C3 double bond of the six-membered ring, an important feature realized in all the compounds (PYR1–8).³¹ There are two potential hydrogen bond donors, namely H1N and H2N and two potential acceptors, namely sulfur atom S1 and carbonyl oxygen atom O1. The crystal structure is stabilized by N–H \cdots O=C, involving H1N, forming molecular chains along the crystallographic *a* axis, followed by N–H \cdots S=C dimers,³² involving H2N in the *ab* plane, giving rise to a sheet like structure (referred to as a “polar sheet” involving polar functional groups). There are two characteristic distances **d1** and **d2** [Fig. 3] which separate the polar sheets in the crystal packing (across the center of symmetry). The distance **d1** is almost invariant in all the crystal structures analyzed here, whereas **d2** depends on the size and nature of the functional group (whether it is involved in intermolecular interactions) present on the phenyl moiety (termed “hydrophobic spacer”). The distance **d1** and **d2** between two consecutive sheets is $\sim 3.758 \text{ \AA}$ and $\sim 8.267 \text{ \AA}$. The void between the sheets is stabilized by aromatic $\pi\cdots\pi$ stacking interaction between the aromatic fluoro-phenyl moieties, the distance between adjacent rings being ~ 3.510 and $\sim 3.620 \text{ \AA}$ respectively. Furthermore, C–H \cdots F interactions provide additional stability to the crystal packing.³³

Table 1 Relevant crystallographic data

DATA	PYR1 (<i>p</i> -F)	PYR2 (<i>o</i> -Cl)	PYR3 (<i>m</i> -Cl)	PYR4 (<i>p</i> -Me)	PYR5 (<i>p</i> -NMe ₂)	PYR6 (<i>p</i> -OMe)	PYR7 (<i>m</i> -OMe)	PYR8 (<i>tris</i> -(OMe) ₃)
Formula	C ₁₄ H ₁₅ FN ₂ O ₂ S	C ₁₄ H ₁₅ ClN ₂ O ₂ S	C ₁₄ H ₁₅ ClN ₂ O ₂ S	C ₁₅ H ₁₈ N ₂ O ₂ S	C ₁₆ H ₂₁ N ₃ O ₂ S	C ₁₅ H ₁₈ N ₂ O ₃ S	C ₁₅ H ₁₈ N ₂ O ₃ S	C ₁₇ H ₂₂ N ₂ O ₅ S
CCDC Number	732835	734014	732837	732836	738484	732834	734015	732838
Formula weight	294.35	310.80	310.80	290.38	319.43	306.38	306.38	366.44
Color	colorless blocks	colorless rod	colorless plates	colorless blocks	colorless plates	colorless plates	colorless rod	colorless blocks
Crystal morphology	0.32 × 0.28 × 0.22	0.28 × 0.20 × 0.14	0.32 × 0.23 × 0.18	0.34 × 0.27 × 0.15	0.25 × 0.15 × 0.10	0.32 × 0.28 × 0.21	0.32 × 0.28 × 0.18	0.42 × 0.32 × 0.28
Crystal Size/mm	292	292	292	292	292	292	292	292
<i>T</i> /K	292	292	292	292	292	292	292	292
Radiation	Mo-K α	Mo-K α	Mo-K α	Mo-K α	Mo-K α	Mo-K α	Mo-K α	Mo-K α
Wavelength/Å	0.71073	0.71073	0.71073	0.71073	0.71073	0.71073	0.71073	0.71073
Crystal system	Triclinic	Triclinic	Triclinic	Triclinic	Triclinic	Monoclinic	Monoclinic	Triclinic
Space group	<i>P</i> 1	<i>P</i> 1	<i>P</i> 1	<i>P</i> 1	<i>P</i> 1	<i>C</i> 2/ <i>c</i>	<i>P</i> 2 ₁ / <i>n</i>	<i>P</i> 1
<i>a</i> /Å	7.347(2)	11.534(5)	7.294(3)	7.350(9)	7.369(3)	18.239(2)	12.286(2)	8.0235(3)
<i>b</i> /Å	9.542(3)	12.540(5)	10.430(4)	9.4652(12)	9.4420(19)	7.3435(8)	8.2534(10)	10.6374(5)
<i>c</i> /Å	11.327(4)	12.618(5)	10.634(4)	12.2073(16)	13.086(3)	25.197(3)	15.956(3)	11.8171(4)
α (°)	71.093(5)	81.012(5)	107.600(6)	74.218(2)	102.79(3)	90.0	90.0	84.489(3)
β (°)	88.642(5)	64.177(5)	90.610(6)	88.672(2)	90.557(19)	101.957(3)	106.98(2)	74.115(3)
γ (°)	69.792(5)	64.737(5)	107.820(6)	69.844(2)	110.68(2)	90.0	90.0	69.045(4)
Volume/Å ³	701.6(4)	1484.7(11)	729.4(5)	765.37(17)	826.8(4)	3301.7(6)	1547.4(5)	905.90(7)
<i>Z</i>	2	4	2	2	2	8	4	2
Density (gms/ml)	1.393	1.390	1.415	1.260	1.283	1.233	1.315	1.343
μ (mm ⁻¹)	0.245	0.400	0.407	0.214	0.206	0.207	0.220	0.208
<i>F</i> (000)	308	648	324	308	340	1296	648	388
θ (min, max)	1.91, 25.99	3.28, 25.00	2.02, 25.00	1.74, 26.00	3.17, 33.84	1.65, 25.00	3.00, 26.00	3.59, 26.00
Total no of refl ⁿ	7222	22805	6999	7983	4460	15282	22076	18202
No. Unique refl ⁿ	2723	5214	2569	2978	3070	2907	3032	3553
No. of parameters	183	365	183	184	203	193	193	231
<i>R</i> _o obs, <i>wR</i> _o obs	0.0413, 0.1121	0.0462, 0.0944	0.0653, 0.1745	0.0418, 0.1113	0.0412, 0.1006	0.0468, 0.1376	0.0494, 0.1189	0.0372, 0.1053
$\Delta\rho_{\text{min}}$ (e Å ⁻³), $\Delta\rho_{\text{max}}$ /e Å ⁻³	-0.242, 0.290	-0.221, 0.199	-0.377, 0.696	-0.200, 0.292	-0.174, 0.291	-0.300, 0.385	-0.217, 0.284	-0.212, 0.218
Goof	1.036	0.864	1.091	1.068	1.036	1.066	0.975	1.115

Table 2 Relevant experimental torsion angles (°)

Torsion	PYR1	PYR2	PYR3	PYR4	PYR5	PYR6	PYR7	PYR8
C9–C4–C3–C5	79.3(2)	59.5(3),65.8(3)	79.2(3)	77.5(2)	79.0(2)	80.0(2)	83.5(2)	69.8(2)
C4–C3–C5–O2	–152.2(2)	6.0(4), 16.3(3)	–161.5(3)	–156.0(2)	–158.2(2)	–160.3(2)	4.2(3)	7.4(2)
C9–C4–N2–C1	93.1(2)	131.8(3),118.2(3)	91.2(3)	92.8(2)	92.1(2)	89.4(2)	90.8(2)	103.5(2)
C14–C9–C4–C3	16.7(2)	–134.9(3),–141.3(3)	12.7(4)	20.6(2)	22.0(2)	25.6(3)	13.0(3)	–139.0(1)
C4–N2–C1–N1	16.1(2)	–4.2(4), 2.8(4)	17.0(4)	–165.4(1)	16.9(3)	19.4(3)	15.1(3)	12.3(2)

Table 3 List of intra- and intermolecular interactions; Cg1 is the center of gravity of the isolated double bond C2=C3; Cg2 is the center of gravity of the six-membered aryl ring C9/C14

Compound	D–H···A	d(D–H)	d(H···A)	d(D···A)	∠(D–H···A)	Symmetry code
PYR1	C14–H14···Cg1	0.93	2.79	3.315(2)	117	x, y, z
	N1–H1N···O1	0.86	2.31	3.102(1)	154	x – 1, y, z
	N2–H2N···S1	0.86	2.50	3.334(1)	165	–x + 1, –y, –z + 1
	N1–H1N···F1	0.86	2.70	3.293(1)	127	–x + 1, –y, –z + 2
	C6–H6B···F1	0.97	2.62	3.415(1)	140	–x + 2, –y, –z + 2
PYR2	C7–H7B···Cg2	0.96	2.71	3.650(1)	165	x, y – 1, z
	C14–H14···Cg1	0.93	2.93	3.364(1)	110	x, y, z
	C14'–H14'···Cg1'	0.93	2.80	3.266(1)	112	x, y, z
	N2'–H2N'···S1	0.86	2.76	3.500(1)	145	x, y, z
	N2–H2N···S1'	0.86	2.54	3.372(1)	164	x, y, z
	C8'–H8'3···O1'	0.96	2.24	2.835(1)	120	x, y, z
	C8–H8A···O1	0.96	2.18	2.896(1)	131	x, y, z
	N1–H1N···S1	0.86	2.60	3.450(1)	169	–x, –y + 1, –z + 1
	N1'–H1N'···S1'	0.86	2.63	3.476(1)	167	–x, –y, –z + 2
	C13–H13···O1	0.93	2.47	3.377(1)	166	–x + 1, –y, –z + 1
PYR3	C14–H14···Cg1	0.93	2.65	3.122(2)	112	x, y, z
	N2–H2N···S1	0.86	2.56	3.393(3)	164	–x + 2, –y + 1, –z + 2
	N1–H1N···O1	0.86	2.12	2.970(3)	169	x + 1, +y, +z
	C12–H12···O1	0.93	2.74	3.621(4)	160	–x + 1, –y + 1, –z + 1
PYR4	C6–H6B···C11	0.97	2.94	3.750(3)	142	–x + 1, –y + 1, –z + 1
	C14–H14···Cg1	0.93	2.67	3.146(2)	113	x, y, z
	N1–H1N···O1	0.86	2.23	3.057(2)	162	x – 1, +y, +z
PYR5	N2–H2N···S1	0.86	2.48	3.323(2)	165	–x + 1, –y, –z + 1
	C7–H7B···Cg2	0.96	2.64	3.581(3)	166	x, y – 1, z
	C14–H14···Cg1	0.93	2.65	3.122(2)	112	x, y, z
	N1–H1N···O1	0.86	2.23	3.060	163	x + 1, +y, +z
PYR6	N2–H2N···S1	0.86	2.49	3.328	165	–x + 1, –y, –z + 1
	C7–H7B···Cg2	0.96	2.58	3.514(3)	163	x, y + 1, z
	C14–H14···Cg1	0.93	2.63	3.120(2)	114	x, y, z
	N1–H1N···O1	0.86	2.13	2.985(2)	170	x, +y – 1, +z
	N2–H2N···S1	0.86	2.50	3.321(2)	159	–x + 1/2, –y + 1/2 + 1, –z + 1
PYR7	C7–H7B···Cg2	0.96	2.70	3.644(4)	168	–1/2 + x, –1/2 + y, z
	C15–H15C···Cg2	0.96	2.94	3.687(4)	136	1/2 – x, 1/2 + y, 1/2 – z
	C14–H14···Cg1	0.93	2.67	3.133(2)	112	x, y, z
	C8–H8A···O1	0.96	2.17	2.875(3)	129	x, y, z
	N1–H1N···S1	0.86	2.52	3.344(2)	162	–x + 5/2, +y – 1/2, –z + 3/2
PYR8	N2–H2N···S1	0.86	2.41	3.249(2)	165	–x + 5/2, +y + 1/2, –z + 3/2
	C12–H12···O1	0.93	2.64	3.525(3)	158	–x + 3/2, +y + 1/2, –z + 3/2
	C7–H7C···Cg2	0.96	2.94	3.724(3)	139	–1/2 + x, 1/2 – y, –1/2 + z
	C14–H14···Cg1	0.93	2.77	3.216(2)	110	x, y, z
	C8–H8A···O1	0.96	2.15	2.880(3)	131	x, y, z
	C17–H17C···O4	0.96	2.48	3.070(3)	120	x, y, z
	N2–H2N···S1	0.86	2.65	3.468(2)	159	–x + 2, –y + 1, –z + 1
	N1–H1N···O3	0.86	2.97	3.686(2)	143	x + 1, +y – 1, +z
PYR8	C8–H8C···O3	0.96	2.62	3.378(2)	136	x + 1, +y – 1, +z
	C15–H15C···Cg2	0.96	2.77	3.590(2)	144	–x, –y, –z + 1

Two such successive pairs of “polar sheets” [Fig. 4(a)] across the inversion center are held together by intermolecular C–H···π interaction (involving H7B) [Fig. 4(b)].

Structure of PYR2

The compound crystallizes in the triclinic space group $P\bar{1}$ with $Z = 4$ ($Z' = 2$; molecule A and B [Fig. 5]) molecules in the unit cell.

It is noteworthy that this molecule exists in a near planar conformation. The carbonyl group C5=O1 of the ester moiety rotates to avoid dipole repulsion with the C–Cl bond. Thus it exists in an *s-cis* conformation with respect to the C2=C3 double bond and is near planar with the six membered dihydropyridimine ring, the dihedral twist being 12.52(2)° and 10.13(2)° for molecules A and B respectively. The planar conformation is stabilized by an intramolecular C–H···O=C hydrogen bond,

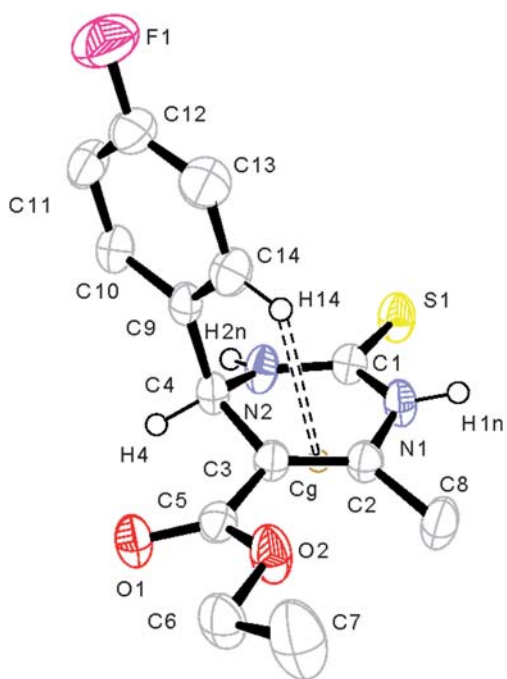


Fig. 2 ORTEP for **PYR1** drawn at 50% ellipsoidal probability. Brown open circle Cg indicates the center of gravity of the double bond C2=C3 and the dotted line depicts C–H... π intramolecular interaction.

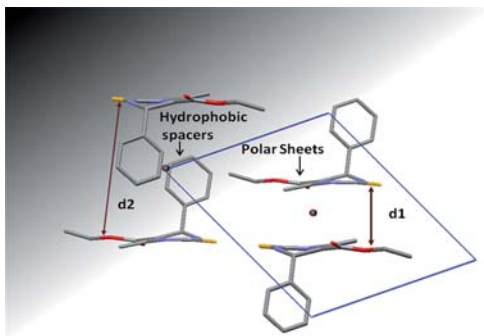


Fig. 3 Crystal packing in 6-methyl-4-phenyl-2-thioxo-1,2,3,4-tetrahydropyrimidine-5-carboxylate ethyl ester, containing the phenyl moiety, depicting the spatial separation between the polar moieties (denoted by **d1**, across the center of symmetry) and the separation **d2** where the hydrophobic moieties separate the consecutive sheets. The blue line indicates the unit cell for a *triclinic* system (as reference for comparison). The colored dots indicate the center of symmetry for the triclinic crystal system.

involving the methyl hydrogen of C8 with the carbonyl oxygen O1 (forming a *S(6)* motif).³⁴ Furthermore, a C–H... π interaction is also present in the existing molecular conformation, between H14 and the C2=C3 double bond of the six-membered ring, thereby locking the molecular conformation [Fig. 5(a)]. It is of interest that the two molecules (A and B) crystallize in the asymmetric unit utilizing N–H...S intermolecular interactions, involving H2N and H2N', not across the center of symmetry. In turn each of the molecules A and B are connected *via* N–H...S=C hydrogen bonds, involving H1N and H1N' forming centrosymmetric dimers. It is noteworthy that molecules [of B

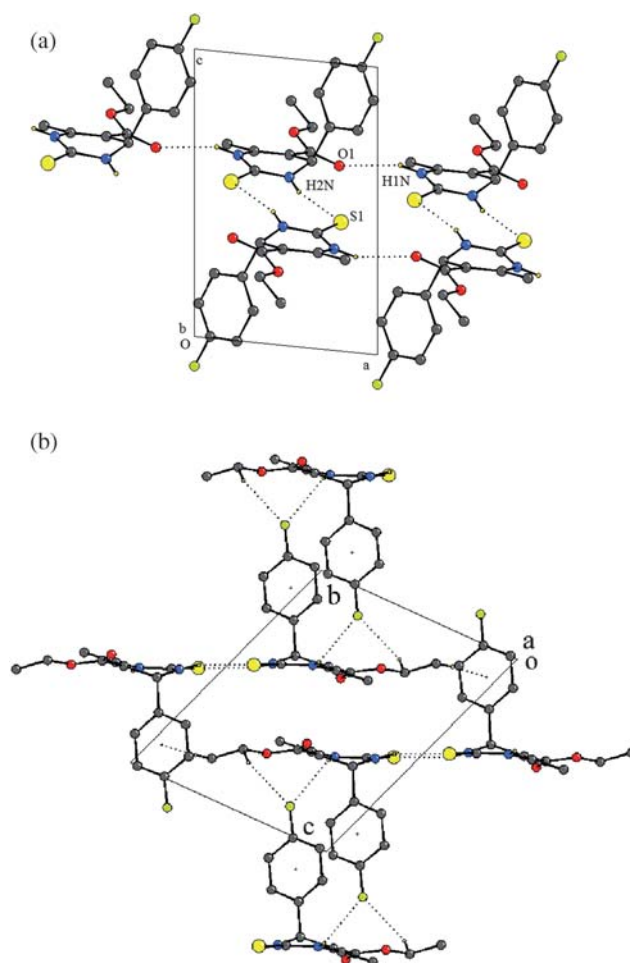


Fig. 4 (a) N–H...S and N–H...O interactions generating a sheet-like structure. The non participating hydrogen atoms have been omitted for clarity. (b) Packing diagram of **PYR1** depicting N–H...S intermolecular dimers along with N–H...F, C–H...F and C–H... π intermolecular interactions. The N–H...O hydrogen bonds are perpendicular to the *bc* plane (along the *a* axis). The non participating hydrogen atoms have been omitted for clarity.

type] form dimeric motifs involving C11...C5=O1 contact and a C11...O2 (ester oxygen) [3.426 Å, 161°; 3.392 Å, 128°] indicating approach of the nucleophilic chlorine towards the electrophilic carbonyl carbon supported by an additional C–Cl...O–C(sp²) contact [Fig. 5(b)].

Structure of **PYR3**

On substitution of the chlorine atom in the *meta* position, the molecular conformation changes to the twisted boat form with concomitant changes in the crystal packing. The molecule crystallizes in the triclinic space group *P* $\bar{1}$ with *Z* = 2 molecules in the unit cell and are iso-structural³⁵ with **PYR1**.

It is of interest to note that the corresponding *para* substituted chlorine compound³⁶ also crystallizes in the same space group (same *Z*), and has similar packing characteristics with **PYR3**. The ester group exists in the *s-trans* orientation with respect to the double bond and out of plane with the tetrahydropyrimidine ring [Fig. 6(a)], the dihedral twist being 14.71(2)°. N–H...O=C

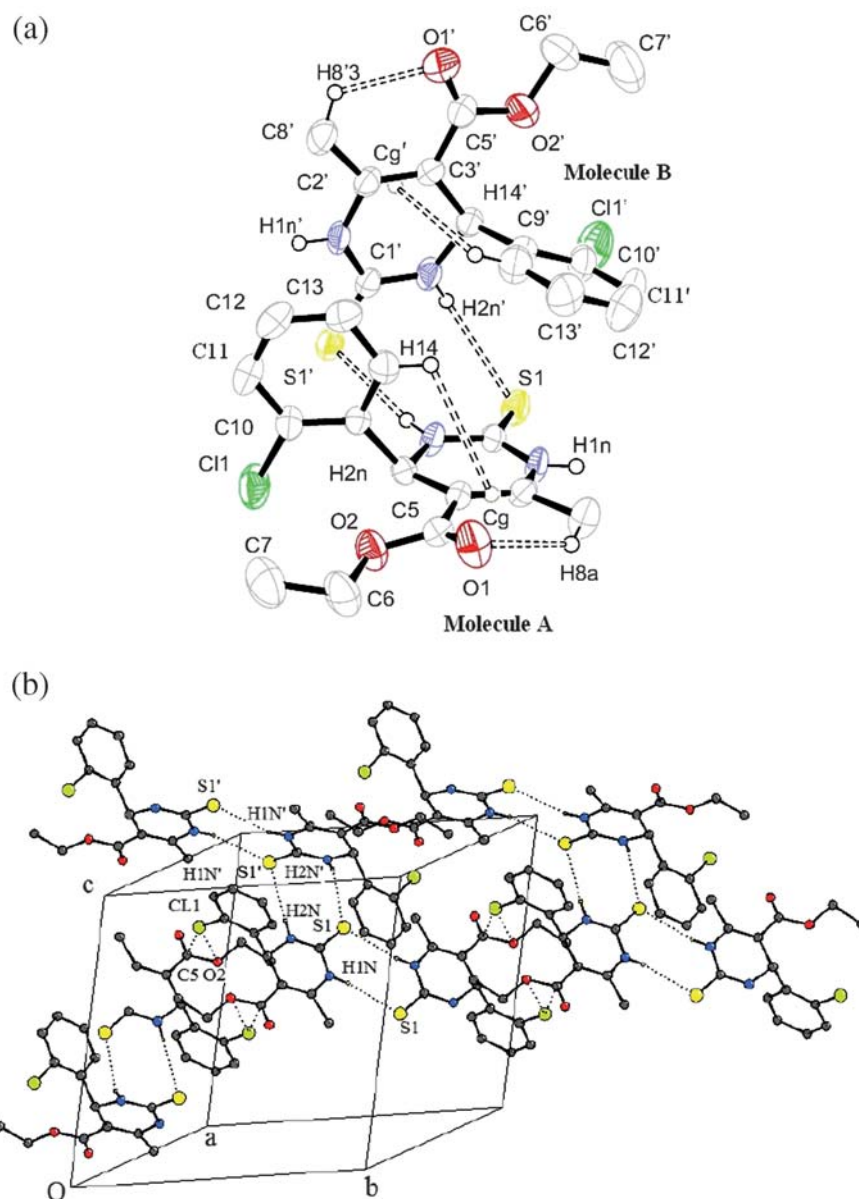


Fig. 5 (a) ORTEP for **PYR2** drawn at 50% ellipsoidal probability. Brown open circle **Cg** and **Cg'** indicates the center of gravity of the double bond $C2=C3$ and $C2'=C3'$ and the dotted line depicts $N-H\cdots S$ intermolecular interaction between the molecules **A** and **B** (asymmetric unit) and $C-H\cdots\pi$ intramolecular interaction respectively in the individual molecule. The ester moiety exists in *s-cis* orientation with respect to the $C2=C3$ double bond. (b) Packing diagram of **PYR2** depicting $N-H\cdots S=C$ interactions involving $H2N$ and $H2N'$ between molecules **A** and **B** (in the asymmetric unit) followed by self dimer formation, via $N-H\cdots S=C$ interactions, involving $H1N$ and $H1N'$, between either **A** and **B** molecules along with short $Cl\cdots C=O$ and $Cl\cdots O-C$ contact in the crystalline lattice. The non participating hydrogen atoms have been omitted for clarity.

hydrogen bonded chains act cooperatively with $N-H\cdots S=C$ hydrogen bonded dimers, forming a sheet like structure. The distance $d1$ and $d2$ between two successive sheets is ~ 3.587 Å and ~ 7.891 Å respectively. This distance $d2$ is less compared to **PYR1**. The electrostatic repulsion of the fluorine atom at the *para* position with the aromatic ring is responsible for the $d2$ distance being higher in **PYR1**. Aromatic stacking interactions are observed between the polar layers, with the distance between the aromatic rings (edge-edge) being 3.365 and 3.476 Å respectively. Furthermore, weak $C-H\cdots O=C$ (involving $H12$) and $C-H\cdots Cl$ (involving $H6B$) interactions provide further stability to the crystal packing [Fig. 6(b)].

Structure of **PYR4**

The presence of a non-polar methyl group in the *para* position results in the molecule crystallizing in the triclinic space group $P\bar{1}$ with $Z = 2$ molecules in the unit cell and the crystal structure being isostructural with **PYR1** & **3** and isomorphous with **PYR1**. The ester group exists in *s-trans* orientation with respect to the double bond and out of plane with the tetrahydropyrimidine ring [Fig. 7(a)], the dihedral twist being $19.84(2)^\circ$. The crystal packing is built up from the interplay of hydrogen bonds involving strong donors and acceptors, namely $H1N$ and $H2N$, forming $N-H\cdots O=C$ and $N-H\cdots S=C$ interactions generating a 2D-sheet like

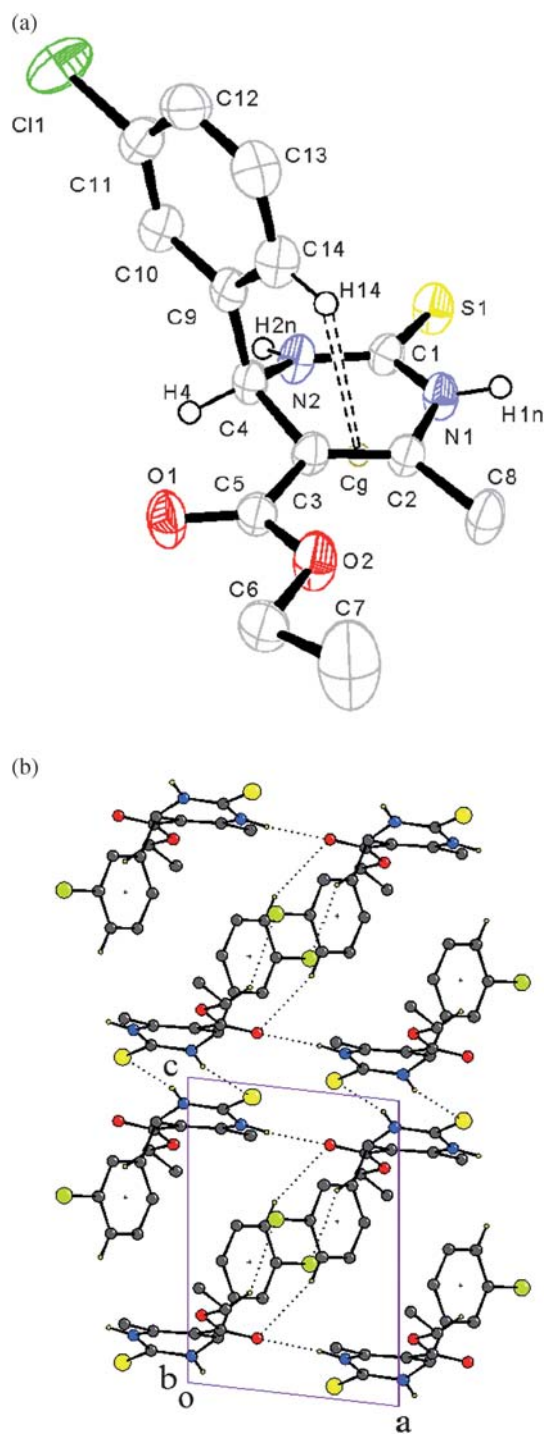


Fig. 6 (a) ORTEP for **PYR3** drawn at 50% ellipsoidal probability. Brown open circle **Cg** indicates the center of gravity of the double bond $C2=C3$ and the dotted line depicts $C-H\cdots\pi$ intramolecular interaction. (b) Packing diagram of **PYR3** depicting $N-H\cdots O$ hydrogen bonds (along *a* axis), $N-H\cdots S$ intermolecular dimers, along with $C-H\cdots O$ and $C-H\cdots Cl$ intermolecular interactions. The non participating hydrogen atoms have been omitted for clarity.

structure. The corresponding distances $d1$ and $d2$ are ~ 4.159 and ~ 9.957 Å between the polar sheets. Successive sheets are stacked, with the aromatic moieties providing additional stability by the formation of $C-H\cdots\pi$ interaction (involving H7B) and displaced

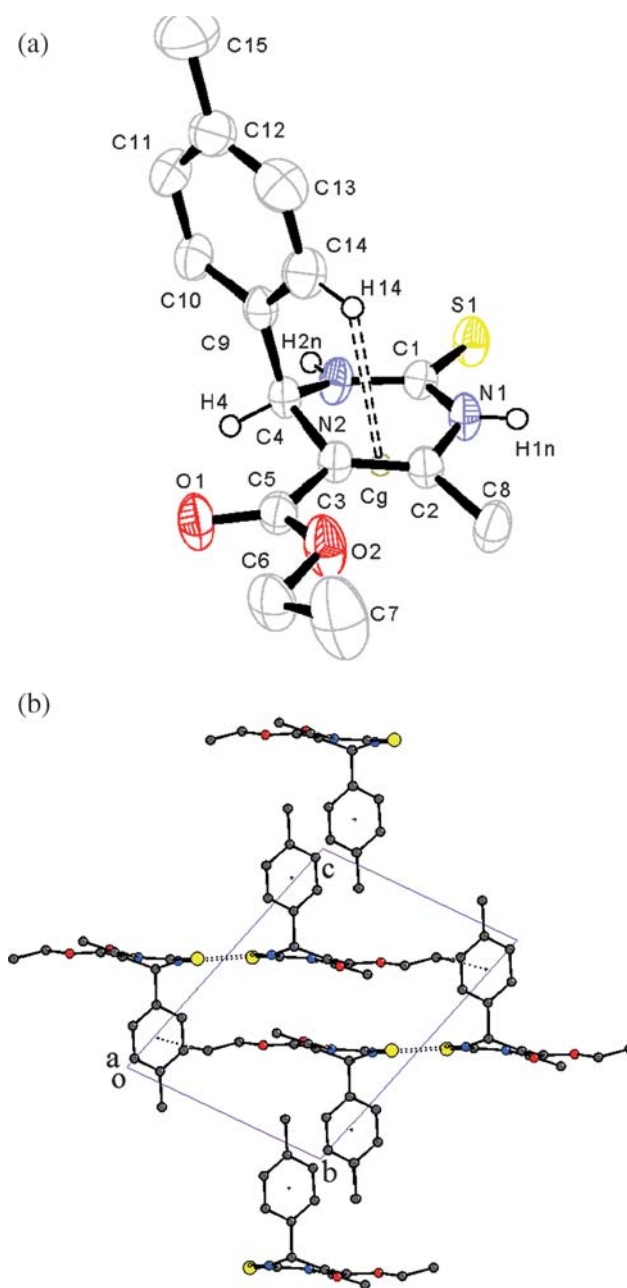


Fig. 7 (a) ORTEP for **PYR4** drawn at 50% ellipsoidal probability. Brown open circle **Cg** indicates the center of gravity of the double bond $C2=C3$ and the dotted line depicts $C-H\cdots\pi$ intramolecular interaction. (b) Packing diagram of **PYR4** depicting $N-H\cdots S$ intermolecular dimers along with $C-H\cdots\pi$ intermolecular interactions. The $N-H\cdots O$ hydrogen bonds are perpendicular to the *bc* plane (along *a* axis). The non participating hydrogen atoms have been omitted for clarity.

edge-to-edge aromatic stacking interactions [Fig. 7(b)] (distance between adjacent aromatic rings being 3.515 and 3.688 Å).

Structure of **PYR5**

The introduction of a *N,N*-dimethyl group in the *para* position [Fig. 8(a)] does not introduce any changes in the molecular conformation and crystal packing. The compound crystallizes in

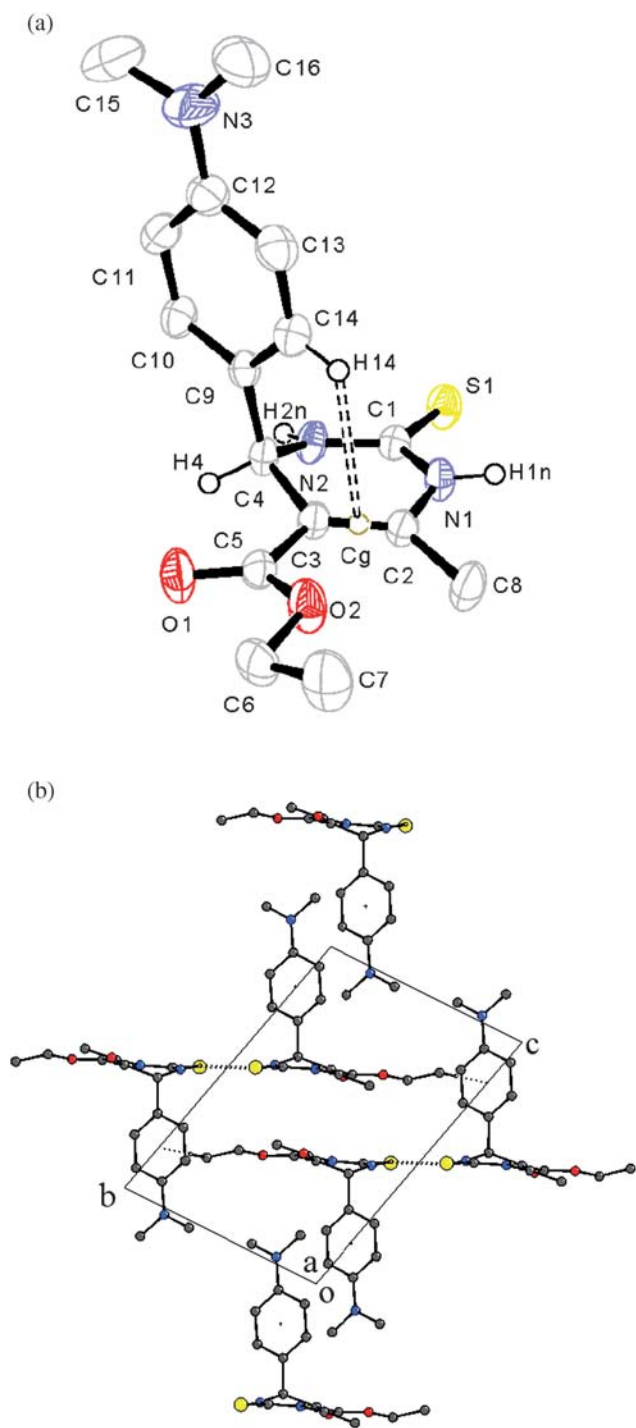


Fig. 8 (a) ORTEP for **PYR5** drawn at 50% ellipsoidal probability. Brown open circle **Cg** indicates the center of gravity of the double bond $C2=C3$ and the dotted line depicts $C-H\cdots\pi$ intramolecular interaction. (b) Packing diagram of **PYR5** depicting $N-H\cdots S$ intermolecular dimers along with $C-H\cdots\pi$ intermolecular interactions. The $N-H\cdots O$ hydrogen bonds are perpendicular to the bc plane (along a axis). The non participating hydrogen atoms have been omitted for clarity.

the triclinic space group $P\bar{1}$ with $Z = 2$ molecules in the unit cell, and are isostructural with **PYR1**, **3** & **4**. The dihedral angle between the pyrimidine ring and the ester moiety is $20.89(2)^\circ$ and exists in *s-trans* orientation with respect to the double bond. The

bond angle $C15-N3-C16$ is $117.9(3)^\circ$ which indicates the absence of pyramidal character of the nitrogen atom $N3$, with the lone pair delocalized over the aromatic phenyl moiety. The crystal structure is built up from $N-H\cdots O=C$ molecular chains and $N-H\cdots S=C$ intermolecular interactions forming dimers, generating a 2D sheet like structure. The distance between the polar sheets $d1$ and $d2$ (sheets containing the non polar aromatic moieties) are $\sim 4.183 \text{ \AA}$ and $\sim 10.265 \text{ \AA}$ [Fig. 8(b)] respectively. This distance $d2$ is higher compared to the previous compounds (**PYR1**, **3** & **4**) because of the greater steric requirements of the N,N -dimethyl group (hydrophobic spacer) which increases the separation between the sheet-like assembly of molecules.

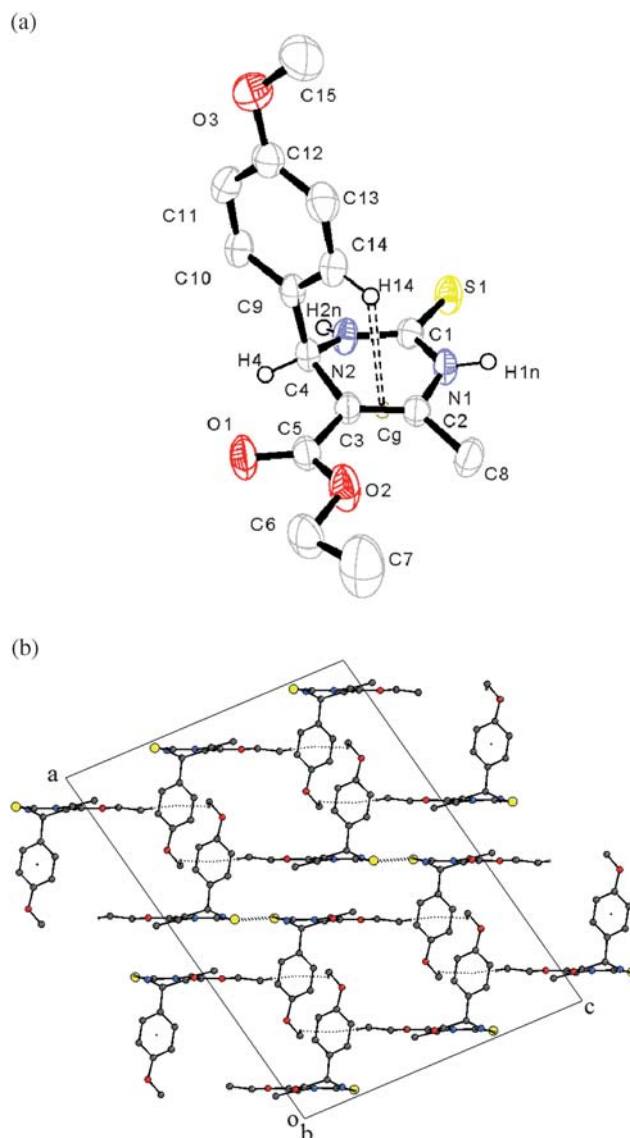
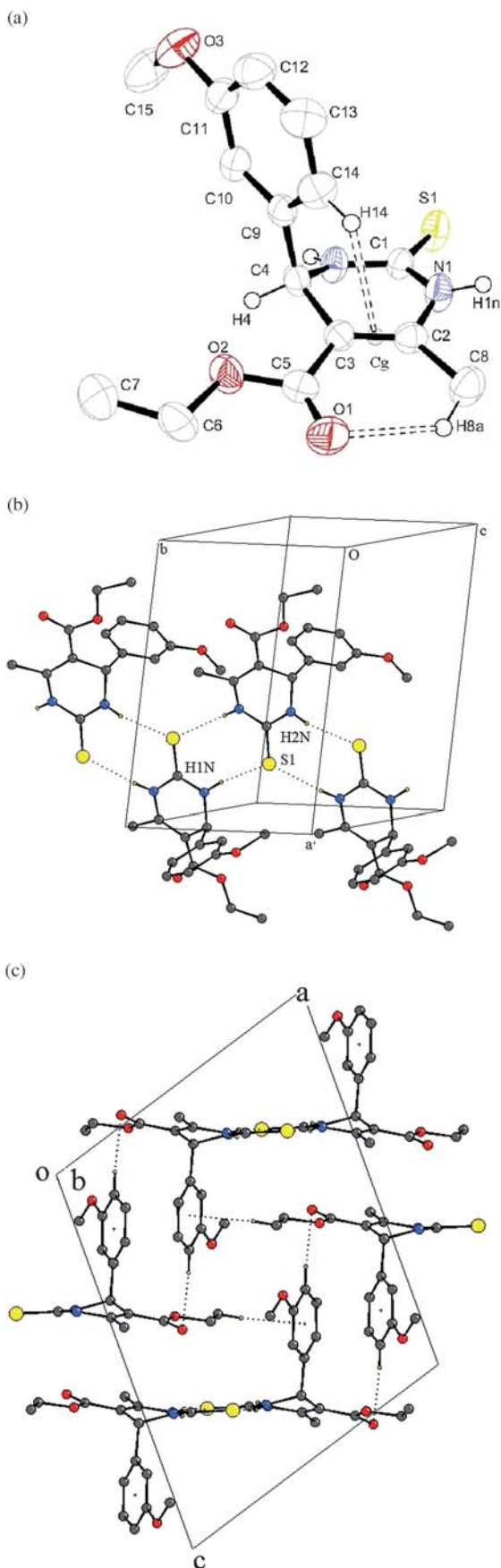


Fig. 9 (a) ORTEP for **PYR6** drawn at 50% ellipsoidal probability. Brown open circle **Cg** indicates the center of gravity of the double bond $C2=C3$ and the dotted line depicts $C-H\cdots\pi$ intramolecular interaction. (b) Packing diagram of **PYR6** depicting $N-H\cdots S$ intermolecular dimers, along with two different $C-H\cdots\pi$ intermolecular interactions, one involving methoxy group and the other a terminal methyl group of ester moiety. The $N-H\cdots O$ hydrogen bonds are along b axis. The non participating hydrogen atoms have been omitted for clarity.



Structure of **PYR6**

The introduction of a methoxy moiety in the *para* position results in the compound [Fig. 9(a)] crystallizing in the monoclinic centrosymmetric space group $C2/c$ with $Z = 8$ in the unit cell. The molecule exists in the twist boat conformation which is further locked by an intramolecular $C-H\cdots\pi$ interaction. It is noteworthy that the crystal packing is controlled by “similar” supramolecular motifs which govern packing of molecules as observed for those of the previous compounds. The $N-H\cdots O=C$ hydrogen bonded chains run along the crystallographic b axis with $N-H\cdots S=C$ forming molecular dimers in the ab plane. The distance $d1$ between the “polar part” of the sheet like structure is $\sim 3.792 \text{ \AA}$ and $d2$ is 10.145 \AA . Due to the role of sterics, the relative orientation of the hydrophobic spacer (*i.e.* the *p*-methoxy phenyl group) is different in the present case. This group rotates and accommodates an intermolecular $C-H\cdots\pi$ interaction, involving H15C, with the aryl moiety, providing stability to the crystal packing. Furthermore, it is noteworthy, that intermolecular $C-H\cdots\pi$ interaction, involving H7B, *i.e.* the terminal hydrogen of the C7 methyl group of the ester moiety, links adjacent sheets together across the inversion center [Fig. 9(b)].

Structure of **PYR7**

On changing the position of the methoxy group from the *para* to the *meta* position on the phenyl ring, it is observed that the orientation of the ester moiety becomes *s-cis* with respect to the double bond, the conformation being stabilized by an intramolecular $C-H\cdots O=C$ interaction, involving H8A (forming a $S(6)$ motif), followed by an intramolecular $C-H\cdots\pi$ interaction [Fig. 10(a)]. The compound crystallizes in the monoclinic $P2_1/c$ space group with $Z = 4$ molecules in the unit cell. The crystal packing is dictated by heterodimeric motifs utilizing $N-H\cdots S=C$ intermolecular hydrogen bonds, involving H1N and H2N forming a $R^2_2(8)$ ring motif generating ribbons [Fig. 10(b)] along the b axis. Furthermore, $C-H\cdots O=C$ involving H12, forms chains along the crystallographic 2_1 screw axis and $C-H\cdots\pi$, involving H7C, *i.e.* the terminal hydrogen of the C7 methyl group of the ester moiety, forming chains along the c glide plane, provide additional stability to the crystal packing [Fig. 10(c)].

Structure of **PYR8**

The compound crystallizes in the triclinic space group $P\bar{1}$ with $Z = 2$ molecules in the unit cell [Fig. 11(a)]. The presence of three methoxy substituents on the phenyl ring results in a flattened boat conformation for the six-membered tetrahydropyrimidine

Fig. 10 (a) ORTEP for **PYR7** drawn at 50% ellipsoidal probability. Brown open circle Cg indicates the center of gravity of the double bond $C2=C3$ and the dotted line depicts $C-H\cdots O$ and $C-H\cdots\pi$ intramolecular interaction. The ester moiety exists in *s-cis* orientation with respect to the $C2=C3$ double bond. (b) The ribbon motif formed using $N-H\cdots S$ intermolecular interactions in **PYR7**. The non participating hydrogen atoms have been omitted for clarity. (c) Packing diagram of **PYR7** depicting $C-H\cdots O$ and $C-H\cdots\pi$ intermolecular interactions. The $N-H\cdots S$ intermolecular dimers forming a ribbon motif, are perpendicular to the b axis. The non participating hydrogen atoms have been omitted for clarity.

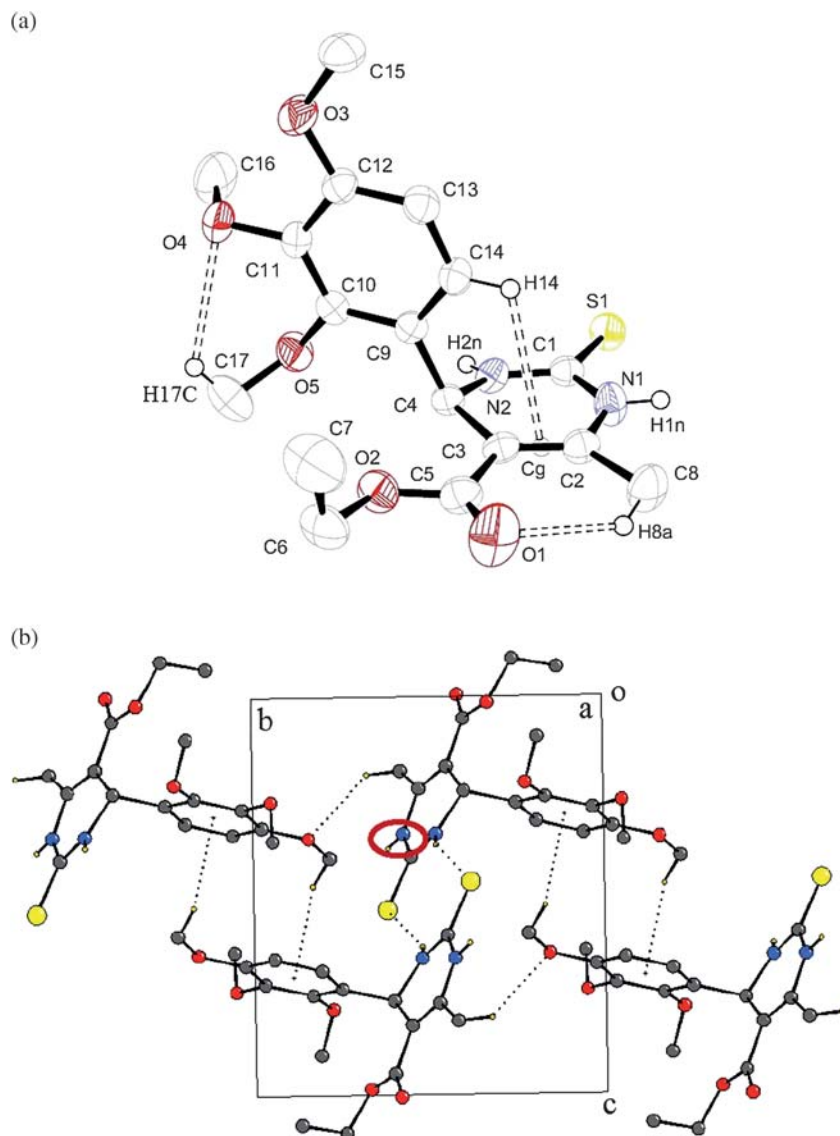


Fig. 11 (a) ORTEP for **PYR8** drawn at 50% ellipsoidal probability. Brown open circle **Cg** indicates the center of gravity of the double bond $C2=C3$ and the dotted line depicts $C-H\cdots O$ and $C-H\cdots\pi$ intramolecular interaction. The ester moiety exists in *s-cis* orientation with respect to the $C2=C3$ double bond. (b) Packing diagram of **PYR8** depicting $N-H\cdots S$ intermolecular dimers, along with $C-H\cdots O$ and $C-H\cdots\pi$ intermolecular interactions. The brown circle indicates the absence of $N-H\cdots O$ hydrogen bonding despite the presence of a potential $N-H$ donor (shown in dark red). The non participating hydrogen atoms have been omitted for clarity.

ring. The total puckering amplitude (Q) is halved with respect to the other molecules **PYR 1–7** (except **PYR2**, Table S3†). Furthermore, the deviations of the flagpole atoms, **N1** and **C4** are also one-third and one-half for this conformation when compared to those observed in the other molecules, except **PYR2** (Table 2). The orientation of the ester moiety is *s-cis* with respect to the double bond. Intramolecular short $C-H\cdots O$ contacts (involving **H8A** and **H17C**) and a $C-H\cdots\pi$ contact are observed in the existing molecular conformation. The three methoxy groups are oriented away from each other in order to minimise the steric repulsions between the hydrogen atoms. The **C6–C7** (ethyl moiety of the ester group) rotates in order to avoid steric repulsion with the **C17** methyl group. The increase in steric bulk, by incorporation of methoxy substituents, results in the absence of a possible $N-H\cdots O=C$ hydrogen bond, between **H1N** and **O1**

due to increased steric and electrostatic repulsion when two symmetry related molecules approach each other. Instead, $N-H\cdots S=C$ intermolecular hydrogen bonds form dimers in the *bc* plane. Another dimer is formed *via* intermolecular $C-H\cdots\pi$ interactions, involving **H15C**, belonging to one of the methoxy groups. These are held together by $C-H\cdots O-C$ (aromatic, sp^2) interaction, involving **H8C** and **O3** forming a trimeric motif in the crystal lattice [Fig. 11(b)]. Thus the crystal packing is a subtle interplay of strong and weak interactions.

Discussions and comparison with related structures in the CSD

A detailed crystallographic investigation of all the substituted tetrahydropyrimidine derivatives enables an understanding of

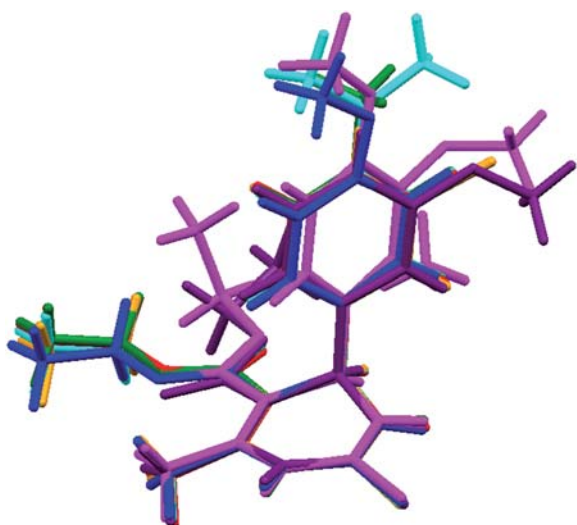


Fig. 12 Overlay diagram depicting the molecular conformation of all the compounds with respect to the tetrahydropyrimidine ring.

the key supramolecular features and intermolecular contacts which pre-organize the molecules and contribute towards the stability of the crystalline lattice. All the above crystal structures display similarities in crystal packing and conformational features. Fig. 12 highlights the overlay diagram depicting differences in molecular conformation due to varying substituents on the phenyl ring. Due to the delocalization of the lone pair of electrons on either of the nitrogen atoms N1 and N2 over the C=S functional group the nitrogen atoms acquires positive charge and the sulfur atoms acquire considerable negative charge.³² This results in the hydrogen atoms attached to these nitrogen atoms being highly acidic. The control and pre-organization of the molecules is utilizing typically strong hydrogen bonded motifs, involving these acidic hydrogens, the common motif being the existence of a N–H···S=C hydrogen bond forming dimeric motifs, further stabilized by N–H···O=C molecular chains generating a sheet like structure. The crystal structures can be separated into two different supramolecular motifs, one built up utilizing strong hydrogen bonds involving polar functional groups, and another built up using hydrophobic moieties. The comparison of related crystal structures in the CSD with the current compounds is performed on the invariant molecular scaffold which is the ethyl-6-methyl-4-phenyl-2-thioxo-1,2,3,4-tetrahydropyrimidine-5-carboxylate core.

The first member of comparison is the crystal structure of **FEDROW**,³⁷ containing a methyl group instead of a phenyl group, and is also isostructural with **PYR 1, 3, 4, 5** compounds. The crystal structure is stabilized by N–H···S=C dimers in the *ac* plane. These are linked with the adjacent dimers by N–H···O=C hydrogen bonds forming C(6) chains along the crystallographic *c* axis forming a sheet like structure. These polar sheets are separated by a distance *d*1 of ~3.534 Å with the adjacent layers related by an inversion center. The space between two successive layers is occupied by the methyl group which exists in axial orientation in the flattened boat conformation. When the methyl group is replaced by a phenyl group (**PESSIQ**),³⁸ it is still isostructural with **PYR 1, 3, 4, 5** compounds having identical packing characteristics, consisting of voids between the polar sheets and edge-

to-edge interactions between the aromatic moieties. The key structural feature is the alteration in the distance between two consecutive polar sheets, one where these directly face each other [*d*1] and the other where the hydrophobic moieties face each other [*d*2], each related by an inversion center. This distance is ~3.424 Å and ~7.885 Å respectively. On substitution of a bromo group at the *para* position on the phenyl ring (**NUQSOH**),¹⁹ the corresponding distances are ~3.807 Å and ~10.358 Å respectively. The space between the layers is further stabilized by highly directional Br···O=C contacts (of the ester moiety) [*d* = 3.367 Å, 161°]. On introduction of a nitro group in the *meta* position on the phenyl ring, these distances are close to those observed in **PESSIQ** with the distances being ~3.742 Å and ~8.010 Å respectively. The aromatic moieties stack in an edge-to-edge fashion, the distance between the aromatic moieties being ~3.412 Å. The distance is less compared with **PESSIQ**, because of the electron withdrawing mesomeric effect of the nitro group which reduces the electrostatic repulsion between the phenyl rings. A comparison of these structures with **XILZUO**³⁹ (hydroxyl in *para* and methoxy in *meta* position) generates a ribbon motif held by N–H···S=C interactions forming dimers in the solid state. It is noteworthy, that identical packing characteristics are also observed in **PYR 7** (the presence of methoxy group “only” in the *meta* position). The increase in the steric bulk on the phenyl group also results in reduced edge–edge interactions between the aromatic moieties, the distance increasing to ~3.727 Å. The distances *d*1 and *d*2 are ~3.743 Å and ~7.748 Å respectively. The distance *d*2 is shorter than the distance observed in **PESSIQ** because of the strong intermolecular C(sp²)-O–H···O=C hydrogen bond between the hydroxyl group and the ester moiety. The presence of only a hydroxyl group on the *para* (**NUQSUN**)¹⁹ and *meta* (**QICTIF**)⁴⁰ position results in a different orientation for the ester moiety (similar to that observed in **PYR8**). The crystal packing is also different because of the participation of the hydroxyl group as a donor and an acceptor in molecular recognition.

Conclusions

In this article, we report the synthesis and characterization of eight differently substituted tetrahydropyrimidine derivatives (varying in functional group substitution on the phenyl ring). The compounds **PYR1-7** (except **PYR2**) exist in the boat conformation and a short intramolecular C–H···π contact characterises this molecular conformation, a feature which has not been recognized in previously studied tetrahydropyrimidine derivatives. This interaction exists between the aromatic ring proton and the double bond of the six-membered ring in conjugation with the ethyl ester moiety. The conformation of the ethyl ester moiety can either be in a *s-cis* or *s-trans* orientation, the latter being the preferred conformation, a subtle interplay due to both electronic and steric effects. The crystal packing is dictated by two primary structural motifs, namely N–H···S=C and N–H···O=C intermolecular hydrogen bonds forming a sheet like structure with the inter layer region being stabilized by C–H···π intermolecular contacts. **PYR 1, 3, 4, 5** are isostructural and are insensitive towards changes in the functional group on the phenyl ring. It is also noteworthy that related compounds in the CSD have similarity in molecular

conformation and crystal packing while others are extremely sensitive to the nature of substitution on the phenyl ring.

Acknowledgements

Susanta K. Nayak thanks CSIR for research fellowship. We all thank IISc, Bangalore X-ray facility under the DST, India scheme. The authors also thank Ms Mamta Biswal for recording all the ¹H-NMR of the compounds under study.

Notes and references

- 1 E. J. Corey, X.-M. Cheng, *The Logic of Chemical Synthesis*, John Wiley & Sons, Limited, Australia 1995.
- 2 A. M. Rouhi, *Chem. Eng. News*, 2004, **82**(7), 63–65.
- 3 H. C. Kolb, M. G. Finn and K. B. Sharpless, *Angew. Chem., Int. Ed.*, 2001, **40**, 2004–2021.
- 4 C. O. Kappe, *Eur. J. Med. Chem.*, 2000, **35**, 1043–1052.
- 5 E. W. Hurst and R. Hull, *J. Med. Chem.*, 1961, **3**, 215–229.
- 6 T. U. Mayer, T. M. Kapoor, S. J. Haggarty, R. W. King, S. I. Schreiber and T. J. Mitchison, *Science*, 1999, **286**, 971–974.
- 7 T. Kato, *Chem. Abstr.*, 1984, **102**, 132067.
- 8 K. S. Atwal, B. N. Swanson, S. E. Unger, D. M. Floyd, S. Moreland, A. Hedberg and B. C. O'Reilly, *J. Med. Chem.*, 1991, **34**, 806–811.
- 9 B. Jauk, T. Pernat and C. O. Kappe, *Molecules*, 2000, **5**, 227–239 and references therein.
- 10 J. M. Blacquiére, O. Sicora, C. M. Vogels, C. M. Cuperlovic, A. Decken, R. J. Ouellette and S. A. Westcott, *Can. J. Chem.*, 2005, **83**, 2052–2059.
- 11 B. Khanetskyy, D. Dallinger and C. O. Kappe, *J. Comb. Chem.*, 2004, **6**, 884–892.
- 12 C. O. Kappe, *Molecules*, 1998, **3**, 1–20.
- 13 G. C. Rovnyak, S. S. David Kimball, B. Beyer, S. G. Cucinotta, J. D. DiMarco, J. Gougoutas, A. Hedberg, M. Malley, J. P. McCarthy, R. Zhang and S. Moreland, *J. Med. Chem.*, 1995, **38**, 119–129.
- 14 S. Goldmann and J. Stoltefuss, *Angew. Chem., Int. Ed. Engl.*, 1991, **30**, 1559.
- 15 K. J. Schleifer, *Pharm. Pharmacol. Lett.*, 1995, **4**, 162.
- 16 (a) C. O. Kappe, *Tetrahedron*, 1993, **49**, 6937–6963; (b) C. O. Kappe, *Acc. Chem. Res.*, 2000, **33**, 879–888; (c) C. O. Kappe, *QSAR Comb. Sci.*, 2003, **22**, 630–645.
- 17 Cambridge Structural Database Version 5.30, November 2008. The CSD analysis resulted in 14 hits. The crystal structures selected are not polymeric, have no disorder, solvent or free ions. The REF codes obtained are FEDROW, FEDROW01 (redetermination at low temperature), MIYBEC, NUQSOH, NUQSUN, PESSIQ, QICTIF, REWDOM, REWDOM01 (redetermination), TAVPEM, TIMJOP, XILZUO, XISMES (hydrate of NUQSUN) and WIHFOJ respectively. Out of these structures, the ones containing the 6-methyl-4-phenyl-2-thioxo-1,2,3,4-tetrahydropyrimidine-5-carboxylate ester moiety are highlighted in black. All these structures were analyzed using the software Mercury²⁵ for comparison with our structures and identify the differences in molecular geometry, conformation and packing features associated with these compounds.
- 18 C. O. Kappe, W. M. F. Fabian and M. A. Semones, *Tetrahedron*, 1997, **53**, 2803–2816.
- 19 O. V. Shishkin, E. V. Solomovich, V. M. Vakula and F. G. Yaremenko, *Russ. Chem. Bull.*, 1997, **46**, 1838–1843.
- 20 K. Devi, K. N. Venugopala, G. K. Rao and P. N. S. Pai, *InPharm Communique.*, 2008, **1**, 19–24.
- 21 *SMART (V 5.628)*, *SAINTE (V 6.45a)*, *Sadbs*, *XPREP*, *SHELXTL*; Bruker AXS Inc.; Madison, WI, 2004.
- 22 Oxford Diffraction (2009). *CrystAlis CCD and CrystAlis RED*, Version 1.171.33.31. Oxford Diffraction Ltd. Abingdon, Oxfordshire, England.
- 23 G. M. Sheldrick, *Acta Crystallogr., Sect. A: Found. Crystallogr.*, 2008, **A64**, 112–122.
- 24 L. J. Farrugia, WinGX (V 1.70.01), *J. Appl. Crystallogr.*, 1999, **32**, 837.
- 25 L. J. Farrugia, *J. Appl. Crystallogr.*, 1997, **30**, 565.
- 26 C. F. Macrae, I. J. Bruno, J. A. Chisholm, P. R. Edgington, P. McCabe, E. Pidcock, L. Rodriguez-Monge, R. Taylor, J. van de Streek and P. Wood, *J. Appl. Crystallogr.*, 2008, **41**, 466.
- 27 M. J. Nardelli, *J. Appl. Crystallogr.*, 1995, **28**, 659.
- 28 A. L. Spek, *Acta Crystallogr., Sect. D: Biol. Crystallogr.*, 2009, **D65**, 148–155.
- 29 M. J. Frisch, G. W. Trucks, H. B. Schlegel, G. E. Scuseria, M. A. Robb, J. R. Cheeseman, J. A. Jr. Montgomery, T. Vreven, K. N. Kudin, J. C. Burant, J. M. Millam, S. S. Iyengar, J. Tomasi, V. Barone, B. Mennucci, M. Cossi, G. Scalmani, N. Rega, G. A. Petersson, H. Nakatsuji, M. Hada, M. Ehara, K. Toyota, R. Fukuda, J. Hasegawa, M. Ishida, T. Nakajima, Y. Honda, O. Kitao, H. Nakai, M. Klene, X. Li, J. E. Knox, H. P. Hratchian, J. B. Cross, V. Bakken, C. Adamo, J. Jaramillo, R. Gomperts, R. E. Stratmann, O. Yazyev, A. J. Austin, R. Cammi, C. Pomelli, J. W. Ochterski, P. Y. Ayala, K. Morokuma, G. A. Voth, P. Salvador, J. J. Dannenberg, V. G. Zakrzewski, S. Dapprich, A. D. Daniels, M. C. Strain, O. Farkas, D. K. Malick, A. D. Rabuck, K. Raghavachari, J. B. Foresman, J. V. Ortiz, Q. Cui, A. G. Baboul, S. Clifford, J. Cioslowski, B. B. Stefanov, G. Liu, A. Liashenko, P. Piskorz, I. Komaromi, R. L. Martin, D. J. Fox, T. Keith, M. A. C. Y. Al-Laham, Peng, A. Nanayakkara, M. Challacombe, P. M. W. Gill, B. Johnson, W. Chen, W. M. Wong, C. Gonzalez, J. A. Pople, *Gaussian 03, revision B.03*; Gaussian, Inc.: Wallingford, CT, 2004.
- 30 D. Cremer and J. Pople, *J. Am. Chem. Soc.*, 1975, **97**, 1354–1358.
- 31 M. Nishio, Y. Umezawa, K. Honda, S. Tsuboyama and H. Suezawa, *CrystEngComm*, 2009, **11**, 1757.
- 32 P. A. Wood, E. Pidcock and F. H. Allen, *Acta Crystallogr., Sect. B: Struct. Sci.*, 2008, **B64**, 491–496.
- 33 (a) D. Chopra and T. N. Guru Row, *Cryst. Growth Des.*, 2005, **5**, 1679–1681; (b) D. Chopra and T. N. Guru Row, *Cryst. Growth Des.*, 2006, **6**, 1267–1270; (c) D. Chopra and T. N. Guru Row, *CrystEngComm*, 2008, **10**, 54–67; (d) D. Chopra, T. S. Cameron, J. D. Ferrera and T. N. Guru Row, *J. Phys. Chem. A*, 2006, **110**, 10465–10477.
- 34 J. Bernstein, R. Davis, E. L. Shimon and N.-L. Chang, *Angew. Chem., Int. Ed. Engl.*, 1995, **34**, 1555–1573.
- 35 A. Kálmán, L. Párkányi and G. Argay, *Acta Crystallogr., Sect. B: Struct. Sci.*, 1993, **B49**, 1039–1049.
- 36 S. K. Nayak, K. N. Venugopala, D. Chopra, T. Govender, H. G. Kruger, G. E. M. Maguire and T. N. Guru Row, *Acta Crystallogr., Sect. E: Struct. Rep. Online*, 2009, **E65**, o2518.
- 37 **FEDROW**: V. E. Zavadnik, A. D. Shutalev, G. V. Gurskaya, A. I. Stash and V. G. Tsirelson, *Acta Crystallogr., Sect. E: Struct. Rep. Online*, 2005, **E61**, o468.
- 38 **PESSIQ**: Y.-Q. Qin, X. -Y. Ren, T. -L. Liang and F.-F. Jian, *Acta Crystallogr., Sect. E: Struct. Rep. Online*, 2006, **E62**, o5215.
- 39 **XILZUO**: Z.-H. Shang, Y. Xiu and Y.-Y. Lin, *Acta Crystallogr., Sect. E: Struct. Rep. Online*, 2007, **E63**, o4172.
- 40 **QICTIF**: C. O. Kappe, O. V. Shishkin, G. Uray and P. Verdino, *Tetrahedron*, 2000, **56**, 1859.